Relevance of the Heisenberg-Kitaev model for the honeycomb lattice iridates A2IrO3

Yogesh Singh, S. Manni, J. Reuther, T. Berlijn, R. Thomale, W. Ku, S. Trebst, Philipp Gegenwart

Relevance of the Heisenberg-Kitaev Model for the Honeycomb Lattice Iridates A_2IrO_3

Yogesh Singh,[1,2] S. Manni,[2] J. Reuther,[3,4] T. Berlijn,[5,6] R. Thomale,[7] W. Ku,[5,6] S. Trebst,[8] and P. Gegenwart[2]

[1]*Indian Institute of Science Education and Research Mohali, Sector 81, SAS Nagar, Manauli PO 140306, India*
[2]*I. Physikalisches Institut, Georg-August-Universität Göttingen, D-37077, Göttingen, Germany*
[3]*Institut für Theorie der Kondensierten Materie, Karlsruhe Institute of Technology, D-76128 Karlsruhe, Germany*
[4]*Department of Physics and Astronomy, University of California, Irvine, California 92697, USA*
[5]*Condensed Matter Physics and Materials Science Department, Brookhaven National Laboratory, Upton, New York 11973, USA*
[6]*Physics Department, State University of New York, Stony Brook, New York 11790, USA*
[7]*Department of Physics, Stanford University, Stanford, California 94305, USA*
[8]*Institute for Theoretical Physics, University of Cologne, 50937 Cologne, Germany*

Combining thermodynamic measurements with theoretical calculations we demonstrate that the iridates A_2IrO_3 (A = Na, Li) are magnetically ordered Mott insulators where the magnetism of the effective spin-orbital $S = 1/2$ moments can be captured by a Heisenberg-Kitaev (HK) model with interactions beyond nearest-neighbor exchange. Experimentally, we observe an increase of the Curie-Weiss temperature from $\theta \approx -125$ K for Na_2IrO_3 to $\theta \approx -33$ K for Li_2IrO_3, while the ordering temperature remains roughly the same $T_N \approx 15$ K. Using functional renormalization group calculations we show that this evolution of θ and T_N as well as the low temperature zigzag magnetic order can be captured within this extended HK model. We estimate that Na_2IrO_3 is deep in a magnetically ordered regime, while Li_2IrO_3 appears to be close to a spin-liquid regime.

Introduction.—The fundamental importance of the Kitaev model, which describes the highly anisotropic exchange of SU(2) spin-1/2 moments on the honeycomb lattice, has quickly been appreciated for its rare combination of microscopic simplicity and an exact analytical solution [1]. It has also become an archetypal example of a microscopic model that—depending on the spatial anisotropy of its couplings—harbors three of the currently most sought-after collective states in condensed matter physics [2]: a gapless spin liquid with emergent Majorana fermion excitations, a gapped Z_2 spin liquid, and a topologically ordered phase with non-Abelian quasiparticle statistics (in the presence of a magnetic field perpendicular to the honeycomb lattice) [1,3]. Especially, physical realizations of topological states of the latter form which support Majorana fermion zero modes [4] are intensely searched for in various candidate systems including certain fractional quantum Hall systems [5], unconventional superconductors [6], as well as heterostructures of topological insulators, semimetals, or semiconductors with conventional s-wave superconductors [7–9], not only because of their fundamentally new character but also due to their possible application in topological quantum computation proposals [10].

A direct realization of the Kitaev model could provide yet another alternative path to this goal. The first proposals to engineer implementations of the Kitaev model were discussed in the context of optical lattices [11] and superconducting circuits [12]. More recently, it has been put forward that strong spin-orbit coupling in certain Mott insulating transition metal oxides [13,14] could inherently

give rise to Kitaev-type couplings of effective spin-orbital degrees of freedom. Among the best candidate materials are layered iridates of the form A_2IrO_3, which exhibit Mott insulating ground states and where the Ir^{4+} form effective $S = 1/2$ moments as it was recently observed for Na_2IrO_3 [15]. On a microscopic level, it has been argued that the strong spin-orbit coupling in these $5d$ transition metal systems leads to orbital dependent anisotropic in-plane exchange that precisely mimics the Kitaev couplings [13]. For real materials, however, further interactions will inevitably be present and, in particular, one might expect that the original spin exchange is not completely damped and isotropic Heisenberg interactions will compete with the anisotropic Kitaev couplings [14]. Such a Heisenberg-Kitaev (HK) model can be written down in its simplest form as

$$H_{HK} = (1 - \alpha)\sum_{ij} \vec{\sigma}_i \cdot \vec{\sigma}_j - 2\alpha \sum_\gamma \sigma_i^\gamma \sigma_j^\gamma, \qquad (1)$$

where the σ_i are Pauli matrices for the effective $S = 1/2$ and $\gamma = x, y, z$ labels the three different links for each spin of the honeycomb lattice. It has been shown [14] that the isotropic Heisenberg exchange in the first term of model (1) enters as antiferromagnetic coupling, while the anisotropic Kitaev exchange (in the second term) is ferromagnetic. Varying the relative coupling α of the two exchange terms a sequence of three different phases has been found [3,14,16]: a conventional Néel antiferromagnet for $0 \leq \alpha \leq 0.4$, a so-called stripy antiferromagnet for $0.4 \leq \alpha \leq 0.8$, and a spin-liquid state for $0.8 \leq \alpha \leq 1$.

But while the A_2IrO_3 materials have been appreciated from a theory perspective as possible candidate materials to look for Kitaev-like and HK-like physics [13,14,16], there has so far been very limited experimental data available for these layered iridates. For Li_2IrO_3 there have been two conflicting reports [17,18], with one report [17] suggesting paramagnetic behavior between $T = 5$ K and 300 K without any sign of magnetic order, while the second report [18] indicated an anomaly in the magnetic susceptibility below $T = 15$ K, which was also accompanied by a hysteresis between zero-field-cooled and field-cooled data, suggesting glassy behavior. No heat capacity data have so far been available for Li_2IrO_3.

For single crystal Na_2IrO_3 some of us have earlier shown [15] Mott insulating behavior with antiferromagnetic ordering below $T_N = 15$ K. Subsequent resonant magnetic x-ray scattering measurements [19] on single crystals were consistent with either stripy or zigzag magnetic order, with supplementary DFT calculations indicating that zigzag order was the more likely magnetic ground state for Na_2IrO_3. This gave rise to another theoretical puzzle, since the original HK model with nearest-neighbor exchange, i.e., model (1), allows for stripy magnetic ordering but not zigzag order. Finite-temperature calculations [16] for model (1) pointed to another discrepancy with experimental observations, since the theoretical calculations indicated that the competition of the Heisenberg and Kitaev exchanges in model (1) does not lead to a substantial suppression of the magnetic ordering transition with regard to the Curie-Weiss scale and the frustration parameter $f = |\Theta|/T_N$ was found to never exceed $f \approx 2$ [16], while for Na_2IrO_3 experiments indicate $f \approx 8$ [15]. Pieces of this puzzle were recently solved when it was shown that taking into account Heisenberg interactions beyond the nearest-neighbor exchange can indeed stabilize the zigzag ordering pattern [20,21]. For antiferromagnetic exchanges, the latter are also expected to introduce geometric frustration. In the following we will expand this discussion of the role of further neighbor Heisenberg exchange and by providing a detailed comparison of theoretical and experimental results we will establish a microscopic description of the layered iridates A_2IrO_3 in terms of such an extended Heisenberg-Kitaev model.

Quickly summarizing our main results we report magnetic and heat capacity measurements on high quality polycrystalline samples of A_2IrO_3 ($A = $ Na, Li) [22]. Magnetic measurements show local-moment behavior with effective spin $S = 1/2$ moments. Both magnetic and heat capacity measurements show sharp anomalies at $T_N = 15$ K for both materials indicating bulk antiferromagnetic ordering. For both materials our DFT calculations indicate that the most likely magnetic order is of zigzag type. Finite-temperature functional renormalization group (FRG) calculations for an extended HK model including next-nearest (J_2) and next-to-next-nearest (J_3) neighbor

antiferromagnetic Heisenberg interactions are then used to confirm the type of magnetic order, and study the evolution of the Curie-Weiss temperature scale θ, the ordering scale T_N, and the frustration parameter $f = |\theta|/T_N$ as α and the various J's are varied. It must be emphasized that in contrast to the classical phase diagram of the extended Heisenberg-Kitaev model discussed earlier [20] our FRG calculations are performed on the quantum level. We show that the experimentally observed evolution of θ, T_N, and f and the observed magnetic order can all be very well captured within this extended HK model. Comparison of experiments with calculations suggest that while the Kitaev term is small for Na_2IrO_3, the Li_2IrO_3 system with $0.6 \leq \alpha \leq 0.7$ sits quite close to the spin-liquid state in the Kitaev limit $\alpha \geq 0.8$.

Magnetic susceptibility.—The magnetic susceptibility $\chi = M/H$ versus T data for A_2IrO_3 ($A = $ Na, Li) are shown in Fig. 1. The $\chi(T)$ data between $T = 150$ K and 300 K were fit by the Curie-Weiss expression $\chi = \chi_0 + \frac{C}{T-\theta}$ with χ_0, C, and θ as fitting parameters. The fit, shown in Fig. 1 as the solid curve through the data, gives the values $\chi_0 = 3.6(4) \times 10^{-5}$ cm^3/mol, $C = 0.40(2)$ cm^3 K/mol, and $\theta = -125(6)$ K, for Na_2IrO_3 and, $\chi_0 = 8.1(7) \times 10^{-5}$ cm^3/mol, $C = 0.42(3)$ cm^3 K/mol, and $\theta = -33(3)$ K, for Li_2IrO_3, respectively. Assuming a g factor $g = 2$ the above values of C correspond to an effective moment of $\mu_{eff} = 1.79(2)\,\mu_B$ and $\mu_{eff} = 1.83(5)\,\mu_B$, for Na_2IrO_3 and Li_2IrO_3, respectively. These values of μ_{eff} are close to the value $1.74\,\mu_B$ expected for spin $= 1/2$ moments. This local-moment formation along with the insulating resistivity (see Supplemental Material [22]) indicates that like its sister compound Na_2IrO_3, Li_2IrO_3 is indeed a
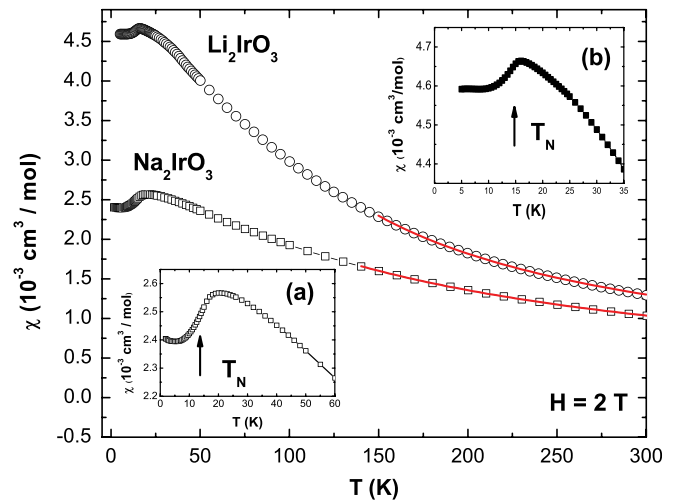

FIG. 1 (color online). Magnetic susceptibility χ versus temperature T for A_2IrO_3 ($A = $ Na, Li). The fit by the Curie-Weiss (CW) expression $\chi = \chi_0 + C/(T - \theta)$ is shown as the curve through the data. The insets (a) and (b) shows the anomaly at the antiferromagnetic ordering for the Na and Li systems, respectively.

Mott insulator. The value of the Weiss temperature $\theta = -33(3)$ K for Li_2IrO_3 further suggests that the effective antiferromagnetic exchange interactions have weakened when compared to the Na_2IrO_3 system. However, the $\chi(T)$ data for Li_2IrO_3 also show an anomaly at 15 K suggesting that an antiferromagnetic transition occurs at roughly the same temperature as for Na_2IrO_3. This is further supported by our heat capacity results presented below. The insets (a) and (b) in Fig. 1 show the $\chi(T)$ data at low temperatures to highlight the anomaly seen at the onset of the antiferromagnetic transition below $T_N = 15$ K in both materials.

Heat capacity.—In Fig. 2 we show heat capacity data divided by temperature C/T versus temperature T for A_2IrO_3 ($A = $ Na, Li), and for the nonmagnetic analog Li_2SnO_3. The anomaly at $T_N = 15$ K in the data for both A_2IrO_3 ($A = $ Na, Li) materials confirms bulk magnetic ordering. A small bump is also observed around $T = 5$ K in the $C(T)$ for Li_2IrO_3. This most likely arises due to a small amount ($\leq 5\%$) of disorder in the sample [23]. The magnetic contribution $\Delta C(T)$ for Li_2IrO_3 shown in the inset of Fig. 2 was obtained by subtracting the $C(T)$ data of Li_2SnO_3 from the data of Li_2IrO_3. The latter reveals a clearly more visible lambda-like anomaly at $T_N = 15$ K. A slight depression of T_N in an applied magnetic field of $H = 9$ T was observed (not shown) which points to the antiferromagnetic nature of the magnetic ordering in Li_2IrO_3. The entropy $S(T)$ obtained by integrating the $\Delta C/T$ versus T data is also shown in Fig. 2 inset. Just above T_N the entropy is only about $15\%R\ln2$. Such a reduced entropy at the transition was also observed earlier for single crystalline Na_2IrO_3 [15]. The small entropy points to the reduced ordered moment and the possible proximity to a nonmagnetic ground state.
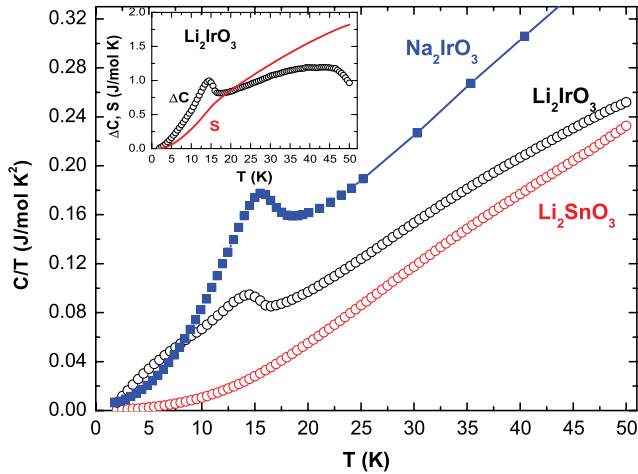

FIG. 2 (color online). Heat capacity divided by temperature C/T versus T data between $T = 1.8$ K and 50 K for A_2IrO_3 ($A = $ Na, Li) and the nonmagnetic analog Li_2SnO_3. The anomaly at $T_N = 15$ K for both A_2IrO_3 materials indicates onset of bulk antiferromagnetic order. The inset shows the difference heat capacity $\Delta C(T)$ and the difference entropy $S(T)$ for Li_2IrO_3.

Magnetic ordering.—From the similarities in the anomalies seen in χ and C data for both the Na and Li systems, it would seem likely that the kind of magnetic order would also be similar for the two. To resolve the magnetic structure for Li_2IrO_3, spin density function calculations within the LDA + U + SO approximation were performed for the Néel, stripy, and zigzag configurations with the moments constrained along the crystallographic axes [18,22]. The results are summarized in Table I. We find that as for Na_2IrO_3 [19], the zigzag configuration has the lowest energy and is hence the most likely magnetic structure for Li_2IrO_3.

We now turn to the evolution of magnetic properties as we go from the Na to the Li compound. From our $\chi(T)$ data above we find that the Curie-Weiss temperature θ decreases from ≈ -120 K to ≈ -33 K on going from Na_2IrO_3 to Li_2IrO_3 possibly indicating that the effective magnetic interactions are weaker for Li_2IrO_3. Surprisingly however, both $\chi(T)$ and $C(T)$ show that both materials order magnetically at roughly the same temperature $T_N \approx 15$ K. The frustration parameter $f = \theta/T_N$, however, reduces from ≈ 8 for Na_2IrO_3 to ≈ 2 for Li_2IrO_3.

In previous theoretical calculations [16] for the thermodynamics of the HK model (1), the ordering temperature T_N was found to be largely insensitive to variations of α whereas θ was found to decrease monotonically with α within the stripy magnetic phase. The increase of the Weiss temperature scale on increasing α is a direct consequence of the fact that the two coupling terms in the HK model (1) enter with opposite coupling signs. Increasing the relative strength of the ferromagnetic Kitaev term thus leads to an increase of the Weiss temperature scale. These theoretical trends thus seem to match well with what is observed in our experiments.

There are, however, two issues where experiments differ from predictions for the HK model. First, the zigzag magnetic order obtained from DFT for both Na_2IrO_3 and Li_2IrO_3 is not one of the three phases of the HK model [14]. Second, a maximum frustration parameter $f \approx 2$ was found in calculations for the HK model [16], which is much smaller than the experimentally observed value $f \approx 8$ for Li_2IrO_3 [15].

To resolve these discrepancies it has recently been argued [20] that further nearest-neighbor antiferromagnetic Heisenberg exchange interactions should be added to the original HK model, which can indeed stabilize the zigzag magnetic order. It was further demonstrated [20] that the experimental magnetic susceptibility data for A_2IrO_3

TABLE I. Total energy E_{tot} per Ir for Li_2IrO_3 for three antiferromagnetic configurations, obtained from collinearly constrained LDA + U + SO simulations.

E_{tot} per Ir(meV)	Zigzag	Stripy	Néel
Li_2IrO_3	0	24	18

(A = Na, Li) materials can only be fit when including the Kitaev term in this expanded microscopic model.

The inclusion of further than nearest-neighbor antiferromagnetic interactions is further expected to introduce geometric frustration in addition to the frustration arising from the competition between the Heisenberg and Kitaev couplings of the original model. We have therefore expanded our FRG calculations [16] to such an extended HK-J_2, J_3 model and determine its thermodynamic properties by extracting the high-temperature CW behavior (from the RG flow), the onset of magnetic ordering (from the breakdown of the RG flow), and the nature of the various ground states by calculating momentum-resolved magnetic susceptibility profiles as further detailed in the auxiliary material [22]. We focused our calculations on the parameter regime $0.2 \leq \alpha \leq 0.8$ and $0 \leq J_2, J_3 \leq 1$. A representative plot of the ordering scale Λ_c as a function of α for fixed $J_2 = J_3 = 0.6$ is shown in Fig. 3 with the inset showing the evolution of the frustration parameter f. Our calculations indicate that zigzag order is stabilized for an extended range $0.25 \leq \alpha \leq 0.7$ in agreement with recent calculations for the HK-J_2, J_3 model [20]. Around the Kitaev limit for $\alpha \gtrsim 0.8$ we find an extended nonmagnetic spin-liquid phase, which connects directly to the one of the original HK model (1). For $\alpha \leq 0.2$ we obtain another nonmagnetic ground state, evidently arising from the further nearest-neighbor exchange J_2, J_3 frustrating the nearest-neighbor J and suppressing the Néel state in favor of a valence bond dimer crystal [21].

Our results summarized in Fig. 3 further indicate that the potentially counterintuitive experimental observation of T_N staying roughly the same in going from Na$_2$IrO$_3$ to Li$_2$IrO$_3$ even though θ decreases by a factor of ≈ 4 in fact agrees well with our calculations showing that the ordering scale stays more or less constant for the zigzag ordered ground state in the regime $0.25 \leq \alpha \leq 0.7$. Finally, we note that our calculations also indicate that the frustration parameter $f = \theta / T_N$ decreases monotonically with α in the region where magnetic order is found (see the inset in Fig. 3), which is a direct consequence of the Curie-Weiss scale θ decreasing monotonically in this region. Interestingly, for small α the geometric frustration induced by the further nearest-neighbor exchange becomes more evident and the parameter f reaches values much larger than obtained for the original HK model [16] and in fact becomes comparable in size to what is observed experimentally for Na$_2$IrO$_3$, where $f \approx 8$.

To place the A_2IrO$_3$ materials on the diagram in Fig. 3 we note that the zigzag ordered ground state indicated in DFT calculations for both materials is found only in the parameter range $0.25 \leq \alpha \leq 0.7$ in the presence of significant second and third neighbor exchange. Additionally, an enhanced frustration parameter f is found only for small $\alpha \gtrsim 0.25$ before the system transitions to a nonmagnetic ground state (for $\alpha \leq 0.2$) and the ordering temperature starts to drop drastically. We therefore place Na$_2$IrO$_3$ at $\alpha \sim 0.25$. In contrast, Li$_2$IrO$_3$ with zigzag order at $T_N = 15$ K and $f \approx 2$ can be placed at $\alpha \gtrsim 0.65$ putting it considerably closer to the spin-liquid regime [24] around the Kitaev limit beyond $\alpha \gtrsim 0.8$.

Finally, we note that in going from the Na to the Li system the a, b lattice parameters are reduced by $\approx 4.5\%$ while the c parameter is reduced by $\approx 10\%$. Thus, substituting Na by Li is equivalent to preferentially applying chemical pressure along the c axis ($\perp$ to the honeycomb planes). This most likely leads to the IrO$_6$ octahedra becoming more symmetrical within the ab plane which in turn enhances the parameters $\eta_{1,2}$ (in the notation of Ref. [14]) leading to an increased Kitaev coupling. This is consistent with the value of $0.6 \leq \alpha \leq 0.8$ estimated above for Li$_2$IrO$_3$ which puts its closer to the Kitaev limit.

In summary, we have shown that magnetic properties of the Mott insulating iridates A_2IrO$_3$, in particular, the evolution of thermodynamic observables, i.e., the Curie-Weiss temperature θ and ordering temperature T_N, as well as their low-temperature magnetic order can be captured within an extended Heisenberg-Kitaev model. Our detailed comparison of experiment and theory, in particular, suggests that while Na$_2$IrO$_3$ is located deep in a magnetically ordered regime, Li$_2$IrO$_3$ lies close to the spin-liquid regime around the Kitaev limit ($\alpha \gtrsim 0.8$). Future experiments will further investigate whether the application of c-axis pressure can push these systems deeper into the orbitally dominated regime, and, in particular, whether Li$_2$IrO$_3$ can be pushed into the spin-liquid phase.
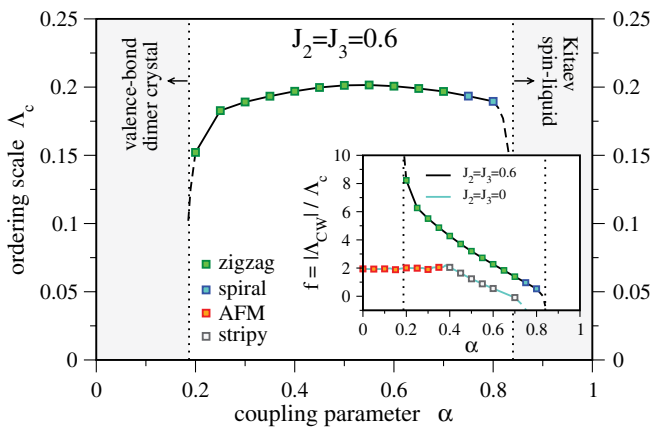
FIG. 3 (color online). Ordering scale Λ_c obtained from the FRG calculations of the HK-J_2, J_3 model as a function of α for J_2, $J_3 = 0.6$. The dashed line indicates the crossover between regions with magnetic order and regions with no long range order at both low and high α, respectively. A regime of enhanced numerical uncertainties is seen near $\alpha \approx 0.8$. The inset shows the frustration parameter f as a function of α for J_2, $J_3 = 0.6$ in comparison to the pure Heisenberg-Kitaev model with J_2, $J_3 = 0$.

Note added in proof.—Very recently, experimental data from inelastic neutron scattering [26] and from neutron diffraction [27] has become available for Na_2IrO_3, which provide direct evidence for zigzag magnetic order. The observed low-energy magnon dispersions [26] further indicate substantial magnetic couplings beyond nearest-neighbor exchange and a relatively weak Kitaev term, possibly due to a substantial deviation from the ideal 90° Ir-O-Ir bonding angle due to trigonal distortions [26,27].

[1] A. Kitaev, Ann. Phys. (N.Y.) **321**, 2 (2006).
[2] L. Balents, Nature (London) **464**, 199 (2010).
[3] H. Jiang *et al.*, Phys. Rev. B **83**, 245104 (2011).
[4] A. Stern, Nature (London) **464**, 187 (2010).
[5] G. Moore and N. Read, Nucl. Phys. **B360**, 362 (1991).
[6] N. Read and D. Green, Phys. Rev. B **61**, 10267 (2000).
[7] L. Fu and C. L. Kane, Phys. Rev. Lett. **100**, 096407 (2008).
[8] J. D. Sau *et al.*, Phys. Rev. Lett. **104**, 040502 (2010).
[9] J. Alicea, Phys. Rev. B **81**, 125318 (2010).
[10] C. Nayak *et al.*, Rev. Mod. Phys. **80**, 1083 (2008).
[11] L.-M. Duan, E. Demler, and M. D. Lukin, Phys. Rev. Lett. **91**, 090402 (2003).
[12] J. Q. You *et al.*, Phys. Rev. B **81**, 014505 (2010).
[13] G. Jackeli and G. Khaliullin, Phys. Rev. Lett. **102**, 017205 (2009).
[14] J. Chaloupka, G. Jackeli, and G. Khaliullin, Phys. Rev. Lett. **105**, 027204 (2010).

[15] Y. Singh and P. Gegenwart, Phys. Rev. B **82**, 064412 (2010).
[16] J. Reuther, R. Thomale, and S. Trebst, Phys. Rev. B **84**, 100406(R) (2011).
[17] I. Felner and I. M. Bradaric, Physica (Amsterdam) **311B**, 195 (2002).
[18] H. Kobayashi *et al.*, J. Mater. Chem. **13**, 957 (2003).
[19] X. Liu *et al.*, Phys. Rev. B **83**, 220403(R) (2011).
[20] I. Kimchi and Y-Z. You, Phys. Rev. B **84**, 180407(R) (2011).
[21] J. Reuther, D. A. Abanin, and R. Thomale, Phys. Rev. B **84**, 014417 (2011).
[22] See Supplemental Material at http://link.aps.org/supplemental/10.1103/PhysRevLett.108.127203 for further details on sample preparation, experimental probes, and theoretical calculations.
[23] S. Manni *et al.* (unpublished).
[24] We note that such a relative placement of the two sister compounds can also be obtained from their relative magnetic susceptibility, which has been studied [25] for the original HK model. It has been predicted that as α varies within the stripy phase, $\chi(T \to 0) \propto \frac{1}{1-\alpha}$. Thus, the higher zero-temperature susceptibility of the Li system, see Fig. 1, indeed points to a higher value of α with regard to the Na system. A more quantitative analysis of the relative zero-temperature susceptibilities, yields $\frac{\chi_{Na}}{\chi_{Li}} \approx 0.5$. Conservatively placing the Na system at $\alpha_{Na} \gtrsim 0.25$, one obtains $\alpha_{Li} \gtrsim 0.63$ consistent with the above estimates from the extended HK model.
[25] F. Trousselet, G. Khaliullin, and P. Horsch, Phys. Rev. B **84**, 054409 (2011).
[26] S. K. Choi *et al.*, following Letter, Phys. Rev. Lett. **108**, 127204 (2012).
[27] Feng Ye, Songxue Chi, Huibo Cao, Bryan Chakoumakos, Jaime A. Fernandez-Baca, Radu Custelcean, Tongfei Qi, O.B. Korneta, and G. Cao, arXiv:1202.3995.